Pergamon

Cement and Concrete Research, Vol. 28, No. 10, pp. 1453–1465, 1998

0008-8846/98 $19.00 + .00

PII S0008-8846(98)00126-4

AGGREGATE-CEMENT PASTE INTERFACE. II: INFLUENCE OF AGGREGATE PHYSICAL PROPERTIES

W.A. Tasong,[1] C.J. Lynsdale,[2] and J.C. Cripps
Centre for Cement and Concrete, Department of Civil and Structural Engineering, The University of Sheffield, Mappin Street, Sheffield, S1 3JD, UK

(Received February 6, 1998; in final form July 23, 1998)

ABSTRACT

This paper describes part of a large project on aggregate-cement interactions and interface bonding mechanisms in concrete. This part of the study investigates the influence of aggregate physical properties on the nature of aggregate-cement paste interfacial bonding with the aim of establishing the bonding mechanisms as controlled by aggregate physical properties. A newly developed experimental technique to characterise quantitatively the aggregate surface texture using a surface profilometer is also presented. Three commonly used concrete aggregate rocks (basalt, limestone, and quartzite) were investigated. Significant differences in the measured bond strength and modes of failure of rock-hardened cement paste composite specimens under uniaxial tension were observed between the different rock types. Based on the results presented, it is apparent that for a given cement paste, the interfacial bond strength cannot be predicted from aggregate surface roughness alone. *© 1998 Elsevier Science Ltd*

Introduction

The increase in demand for high-performance concrete and improved cement-based composites in recent years has resulted in renewed interest in the study of the role of interfaces in composite behaviour. The ITZ is usually regarded as the weakest region in concrete influencing both mechanical properties and durability, and is the reason why the stress-deformation behaviour of concrete differs from that of its individual components, i.e., hydrated cement paste and aggregate.

The importance of aggregate-cementitious matrix interfacial bond has been emphasised by many workers (1–2). It has been suggested (1,3–6) that the bond between aggregate and the cementitious matrix depends on three different mechanisms. These are: the mechanical keying of the hydration products of cement with the rough surface of aggregate (often covered with fine cracks); the epitaxial growth of hydration products at some aggregate

[1]Current address: Centre for Research in the Built Environment, University of Glamorgan, Pontypridd CF37 1DL, United Kingdom.
[2]To whom correspondence should be addressed.

TABLE 1
Summary of rock mechanical and physical properties.

Mechanical and physical properties	Type of rock		
	Basalt	Limestone	Quartzite
Compressive strength (MPa)	158	52	–
Tensile strength (MPa)	10.2	8.4	–
Point load index ($I_{s(50)}$)	4.9	3.9	7.8
Compressive strength obtained from I_s (MPa)	118	94	188
Elastic modulus (GPa)	54	67	–
Aggregate crushing value (%)	22	31	20
Specific gravity	2.80	2.61	2.64
Absorption (%)	1.4	1.3	0.1

surfaces; and the physical-chemical bond between the hydrating cement paste and the aggregate, due to chemical reaction.

Indirect evidence of the bonding mechanisms due to mechanical interlocking aided by the aggregate surface texture has been established (1,2) by comparing the bond strength of fractured rock surfaces with that of polished rock surfaces. However, in these investigations, the true surface area that each aggregate particle presents for bonding (regardless of whether the bond is primarily due to mechanical interlock of cement hydration products with the aggregate surface or a chemical reaction between the aggregate and the cement paste) was either not adequately quantified or not estimated at all. In addition there was often a lack of information about the rock mechanical strength. In order to separate the effects of the individual geological properties of the aggregate on bond strength, it is of vital importance that the total aggregate surface area that is available for bonding is known. However, there is no simple and accurate method available for the quantitative measurement of the surface roughness of aggregate.

Several indirect methods for assessing the surface texture of concrete aggregates are available. These include: the determination of the area covered by a known weight of a suitable medium, such as a fine powder, in building up the surface to a smooth texture; the measurement of air flow between the surface and an elastic barrier held in contact; and the measurement of the dispersion of light incident on the surface (7). These indirect methods have their shortcomings; for instance, they could yield similar results on surfaces on which the irregularities differ in form. Also, direct methods have been proposed in which the irregularities in the surface were themselves measured after being magnified (7). This involves embedding a particle of aggregate in a synthetic resin and obtaining thin sections of the aggregate surrounded by resin. The interface between the aggregate and resin is magnified (125 times) using a projection microscope and traced. The length of the profile obtained is measured by means of a map-measuring wheel and compared with the length of a line drawn as a series of chords. The difference between the two lengths is taken as a measure of the surface roughness. This method has several shortcomings: it is very bulky and time consuming; errors could be introduced during thin section preparation; it is virtually impos-

sible to draw a series chords equal to the true length of the aggregate surface undulations; the test sample needs to be small, and this could result in magnification of errors.

Two-thirds of the volume of concrete consists of aggregate. Hence the development of high-performance concrete requires a fundamental understanding of the influence of aggregate properties on the ITZ. In the present study, an experimental procedure to measure quantitatively the aggregate surface roughness was developed. The effects of aggregate mechanical and physical properties, including surface roughness, on the bond strength at the ITZ were investigated. Evidence that the bond strength depends on the aggregate intrinsic properties and that the interfacial zone is not necessarily the "weakest link" in concrete is presented. The aim of this investigation is to enrich further our understanding of the aggregate-cementitious matrix bonding mechanisms from the viewpoint of aggregate properties, and also to enable advances in the field of high-performance concrete to be made.

Experimental Procedures

Materials

Three typical concrete aggregate rocks, namely basalt, limestone, and quartzite, were chosen for the study. These were selected to have contrasting chemical and physical properties and interactions with the cement paste. The physical and mechanical properties of the rocks are given in Table 1. The cement used was ordinary Portland cement (OPC) complying to BS12. The petrography and chemical composition of the rocks and the OPC are reported elsewhere (8).

Measurements of Surface Roughness of Aggregate

Due to the importance of aggregate surface texture on the bond strength and the lack of a simple and accurate method to measure quantitatively the surface texture of the aggregate, it was felt necessary to develop an experimental procedure to provide suitable data representing the surface roughness of the aggregate used in the investigation.

The basis of the technique chosen is the quantifying of the surface texture (by parameters which relate to certain characteristics of texture) using a surface profilometer (Talysurf 120L by Rank Taylor Hobson, UK) equipped with a stylus and appropriate software as shown schematically in Figure 1. Movement of the stylus is detected by a laser beam, and the technique is capable of measuring changes in topographic heights as small as 0.001 μm. Stylus-type instruments are normally used for the measurement of surface finish of machined metal components. Figure 2 is a schematic representation of the measured parameters, which relate to certain characteristics of texture. These provided data about the textural features listed below. It is worth noting that due to the rough nature of the surface of rock samples (compared to machined metal surfaces) the values reported in Table 2 are rounded to the nearest 0.1 micron.

Parameters

Amplitude Parameters. These include properties such as the arithmetic mean (R_a) of departures of the profile from the mean line, the maximum peak-to-valley height (R_{max}) of the

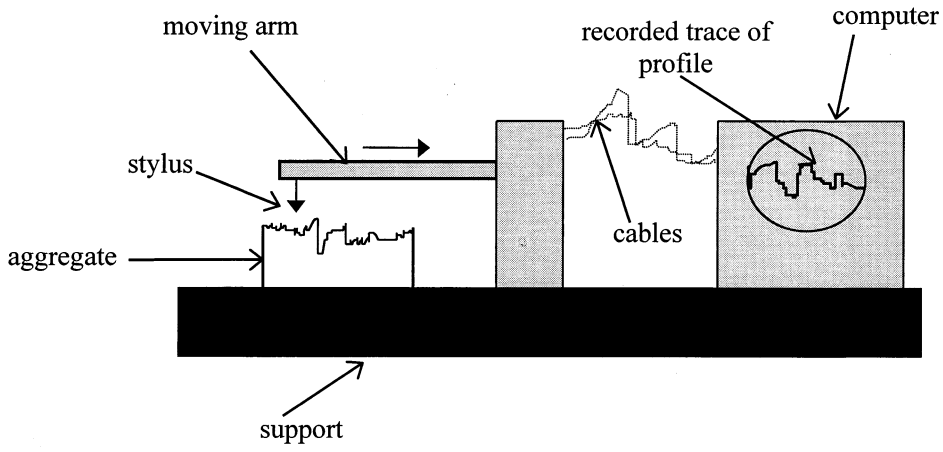

FIG. 1.
Schematic representation of the apparatus used for the aggregate surface roughness.

profile within the sampling length, the average valley height (R_v) below the mean line, the average height difference (R_z) between the five different highest peaks and the five lowest valleys within the assessment length, the maximum height (R_p) of the profile above the mean line within the assessment length, and the skewness (R_{sk}) which is a measure of the symmetry of the amplitude distribution curve about the mean line.

Spacing Parameters. These include the mean spacing (S_m) between profile peaks at the mean line measured over the assessment length.

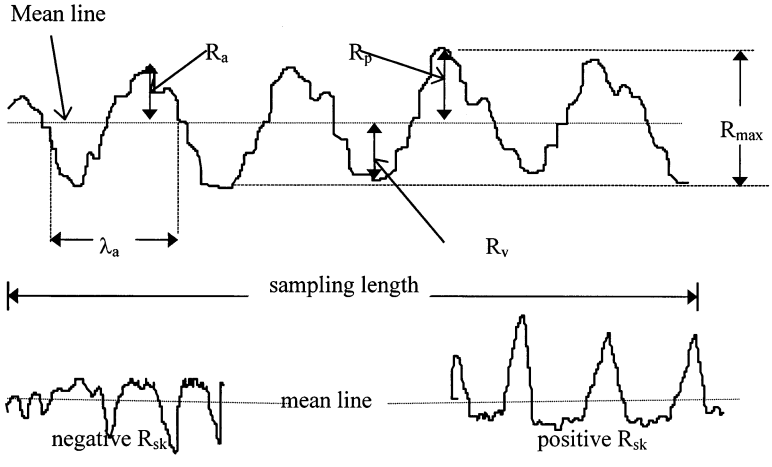

FIG. 2.
Schematic representation of aggregate surface parameters measured.

TABLE 2
Measured parameters that relate to certain characteristics of aggregate surface texture.

	Type of surface								
	Ground surface			Sawn surface			Fractured surface		
Surface parameters	BS	LS	QZ	BS	LS	QZ	BS	LS	QZ
R_a (μm)	4.5	4.7	3.0	5.2	3.5	3.3	171.8	110.0	103.8
R_{max} (μm)	42.0	39.9	30.2	41.8	48.8	30.6	756.0	603.8	466.6
R_p (μm)	8.6	11.1	8.9	11.2	6.8	10.8	354.0	321.4	242.3
R_{sk}	−1.8	−1.2	−1.0	−1.3	−3.2	−0.4	0.0	0.4	0.0
R_z (μm)	32.8	24.8	17.5	33.4	31.0	21.8	**	179.5	**
R_v (μm)	33.4	28.8	21.3	30.6	42.0	19.8	402.0	282.5	224.3
S_m (μm)	153.9	162.9	195.3	113.0	110.0	115.5	2743.5	1533.6	1861.7
Δ_a (degrees)	1.0	−0.7	0.6	0.1	−0.3	−0.5	0.3	2.5	−0.4
λ_a (μm)	36.8	26.6	25.2	31.8	26.7	21.3	196.0	186.3	281.2

Note: BS = basalt; LS = limestone; QZ = quartzite.
** = value exceeded the range of instrument.

Hybrid Parameters. These include the arithmetic mean slope (Δ_a) of the profile throughout the assessment length and the average wavelength (λ_a).

For the purpose of investigating the effects of aggregate surface texture on bond strength, three different aggregate surface finishes were selected, namely, sawn, ground, and fractured. These were chosen to give contrasting physical interactions with the cement paste. The sawn surface texture was obtained by cutting 20 mm cubic pieces of aggregate from the parent rock using a water-lubricated diamond saw. The ground surface texture was obtained by grinding down with size #P240 emery paper previously sawn faces of the 20 mm cubic pieces. Fractured surfaces were obtained by fracturing 20 mm cubes, out of previously sawn 20 × 20 × 200 mm prisms, using a rock splitter.

To measure the surface roughness, the test specimen was mounted in a sample holder and the machine operated by moving the stylus across the surface as shown schematically in Figure 1. Three profiles were taken for each result, two of which were taken along the two diagonals of the 20 mm cubic aggregate while the third was taken centrally.

Measurement of Aggregate-Cement Paste Bond Strength

Due to the difficulties involved in studying ITZ in normal concrete, laboratory specimens were prepared by casting cement paste, with a water/cement ratio of 0.37, against 20 mm aggregate cubes under investigation. The specimens were prepared as shown schematically in Figure 3. This arrangement was chosen to enable the uniaxial tensile bond strength to be measured by pulling the aggregate-cement matrix composite specimens apart in a Hounsefield tensometer with a maximum load capacity of 2.5 kN. The following procedure was adopted to prepare the specimens.

A water-lubricated diamond saw was used to cut out 20 mm cubes of aggregate from the rock. Two 40 mm long threaded metal rods were inserted into both ends of the mould, such

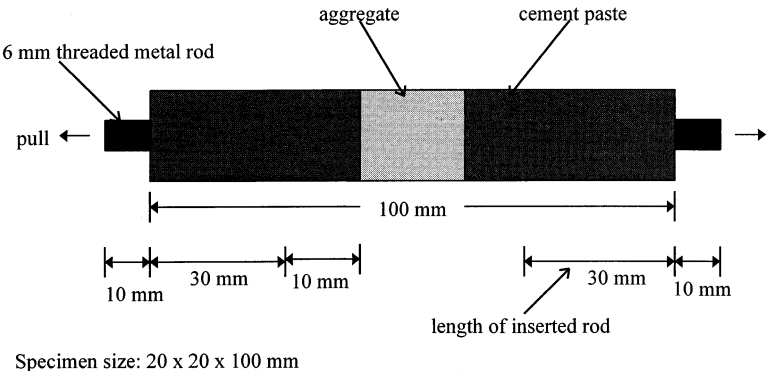

FIG. 3.
Schematic representation of uniaxial tensile bond strength testing apparatus.

that 30 mm extended into the mould. The rods were held in this position using locking nuts. The 30 mm insertion distance was adopted after trial experiments using 20, 25, and 30 mm. During the trial tests, it was observed that when the rod was inserted 20 mm into the paste all the specimens tested failed at the cement paste/rod boundary; when the insertion distance was 25 mm, about 50% of specimens failed at the paste/rod boundary. However, when a 30 mm insertion distance was used, none of the specimens failed at this boundary. It should be noted here that this insertion length depends on the aggregate-cement matrix bond strength.

The specimens were cast in perspex moulds and compacted on a jolting table normally used for testing flow of mortar according to BS 4551:1980. The mould was clamped onto the table and 20 mm cubes of aggregate were placed in the centre of each compartment. A layer of cement paste about 10 mm in thickness was placed on either side of the aggregate in the mould. The table was operated 25 times to compact the layer. The mould was then filled and compacted by operating the table another 25 times. A trowel was used to strike off excess cement paste.

The moulded specimens were covered with a wet woollen cloth and securely covered with polythene in order to keep them moist and prevent shrinkage and cracking at the ITZ. The specimens were left in the laboratory for 24 h, after which time they were demoulded, wrapped in wet cotton cloth, put in sealed polythene bags and stored in a mist room maintained at 21°C and 96% relative humidity until tested. The specimens were tested, at the age of 28 days, in a saturated surface dry conditions in order to prevent shrinkage cracks forming at the ITZ.

Results and Discussion

Aggregate Surface Texture

Typical characteristic surface profiles of ground, sawn, and fractured surfaces of basalt are shown in Figure 4. The surface profiles for limestone and quartzite are not presented here due to space limitation, but a summary of the measured surface parameters is given in Table 2.

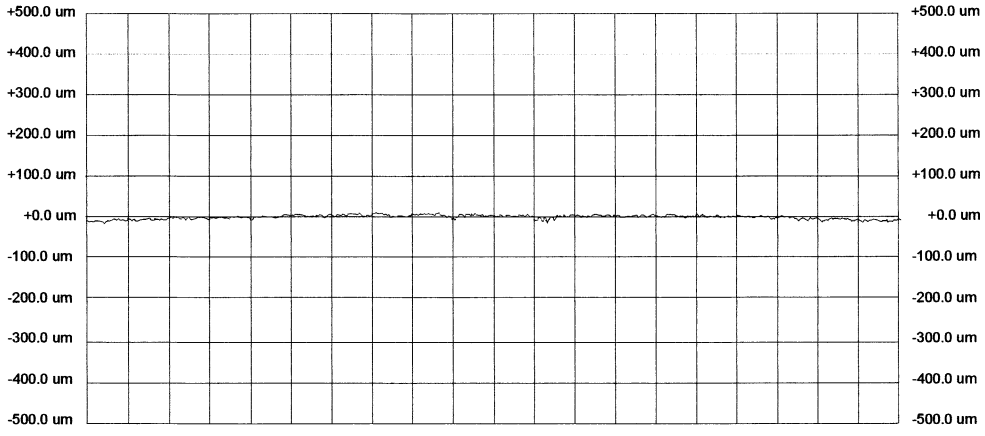

(i) Ground surface of basalt

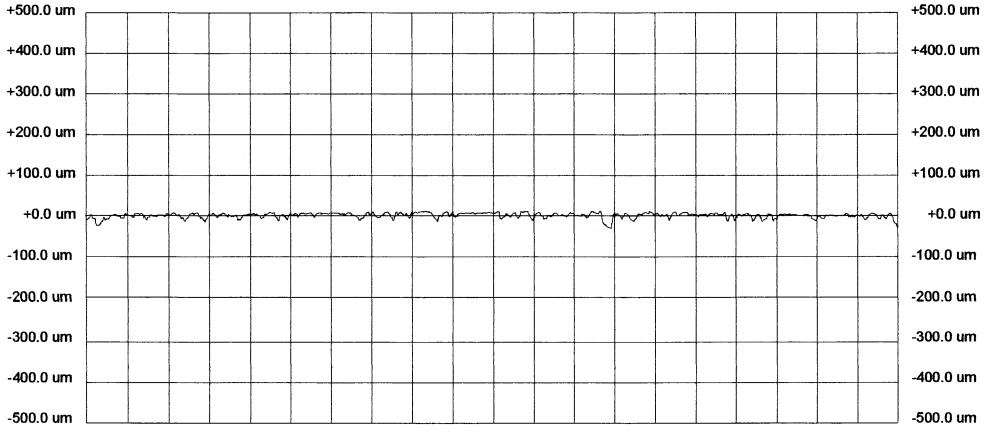

(ii) Sawn surface of basalt

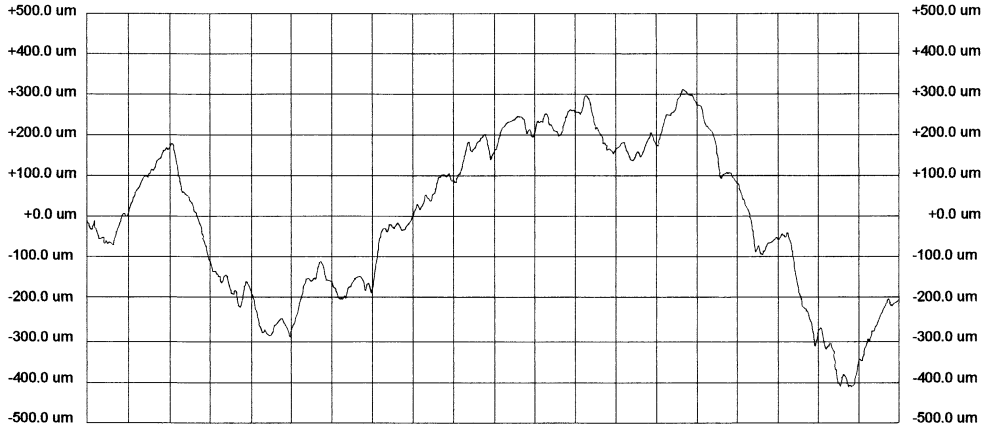

(iii) Fractured surface of basalt

FIG. 4.
Typical charateristic surface profiles of basalt.

These are the average readings for three profiles, two of which were taken along the two diagonals of the 20 mm cubic piece of aggregate while the third was taken centrally.

Theresults (Table 2) show that the measured surface profiles and surface roughness parameters for the ground surfaces are similar for all three aggregates studied, although some minor differences could be observed between the different aggregates.

However, as would be expected, the surface texture characteristics for the sawn aggregate surfaces were observed to differ significantly from those of the ground surfaces. For the sawn surfaces of the limestone and basalt there were no significant differences in the measured profiles and the surface roughness parameters. However, the quartzite aggregate surface roughness value was observed to be lower than those of limestone and basalt. The high hardness of the quartzite rock may be the reason for "weak" saw-marks.

As expected, the surface profile as well as the measured values of the surface parameters were much higher for the fractured aggregate surfaces compared with either the ground or sawn surfaces (Fig. 4 and Table 2). However, there were significant differences between the three rock types studied. The basalt aggregate fractured surface was rougher than that of limestone which was rougher than that of quartzite.

Differences in rock crystalline texture, hardness and intergranular bonding between the minerals grains are possibly the main reasons for the observed differences in surface texture characteristics of the rocks studied. Quartzite produced a conchoidal fracture which resulted in a much smoother surface texture than the other rock types. Meanwhile, the presence of well defined cleavage planes (or planes of weakness) in calcite, the main constituent of the limestone, is considered to be the main reason for the low surface roughness of its fractured surface compared with basalt which breaks with sharper and rougher surfaces, hence its suitability as road surfacing stone.

Effects of Aggregate Surface Roughness on the Nature of the Bond at the ITZ

Four different modes of bond failure in direct tension tests were observed due to differences in mineralogy, structure, and surface features of the rocks used in the investigation and the resulting variation in their interaction with the cement paste. These included:

1. Mode A: Failure crack passed cleanly at the ITZ.
2. Mode B: Failure cracks ran through the ITZ at some points and continued through the paste.
3. Mode C: Failure cracks ran through the ITZ at some points and continued through the aggregate.
4. Mode D: Failure cracks passed through the ITZ as in mode A, but with loose fragments of aggregate particles peeling off to the cement paste side.

As Figure 5 shows, there were significant differences between the three types of rocks in terms of how the rock surface characteristics influenced the nature of the bond at the ITZ. Figures 6 to 10 relate the aggregate surface parameters to the measured tensile bond strength. It should be noted that eight specimens were tested for each result and the coefficient of variation was in all cases less than 5%.

Basalt Aggregate. Unlike limestone and quartzite, the basalt-cement paste interfacial bond strength was observed to increase consistently with increasing surface roughness of the

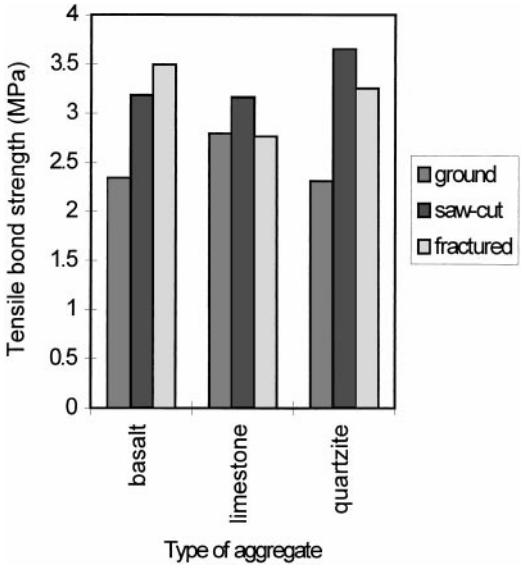

FIG. 5.
Summary of effects of aggregate surface roughness on tensile bond strength.

aggregate. The ground aggregate surface achieved the lowest bond strength, followed by the sawn surface, and both types of surfaces showed the type A mode of failure. On the other hand, the fractured surface achieved higher 'apparent' bond strength and showed the type B mode of failure. A similar mode of failure was reported by Alexander et al. (9) during an investigation into cement paste-andesite rock composite fracture properties. The basalt rock

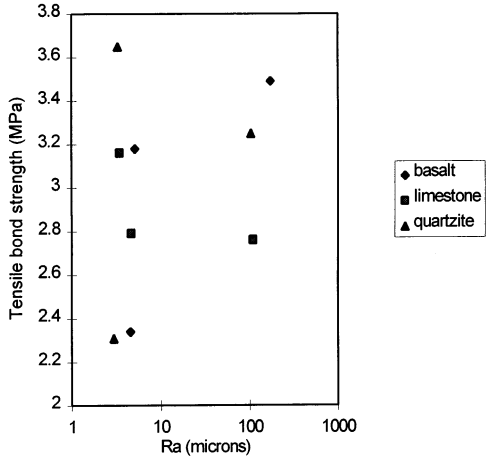

FIG. 6.
The effect of the arithmetic mean (R_a) of departure of the rock aggregate surface profile from the mean line on measured tensile bond strength.

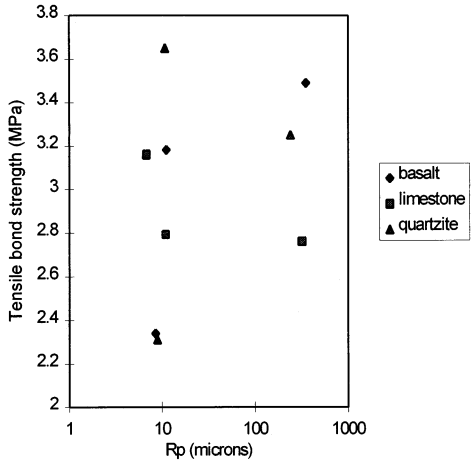

FIG. 7.
The effect of the maximum height (R_p) of the rock aggregate surface profile above the mean line on measured tensile bond strength.

has a firmer or stronger crystalline texture with no zones of weakness and hence the high "apparent" interfacial bond strength achieved by its fractured surface.

Limestone Aggregate. Unlike the basalt aggregate, the limestone aggregate-cement paste interfacial bond strength did not increase consistently with increasing surface roughness of

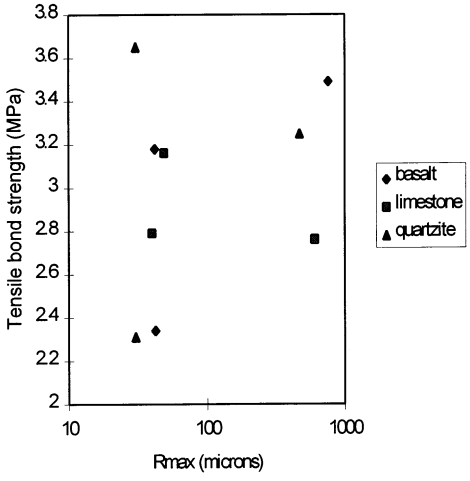

FIG. 8.
The effect of the maximum peak-to-valley height (R_{max}) of the rock aggregate surface within the profile on measured tensile bond strength.

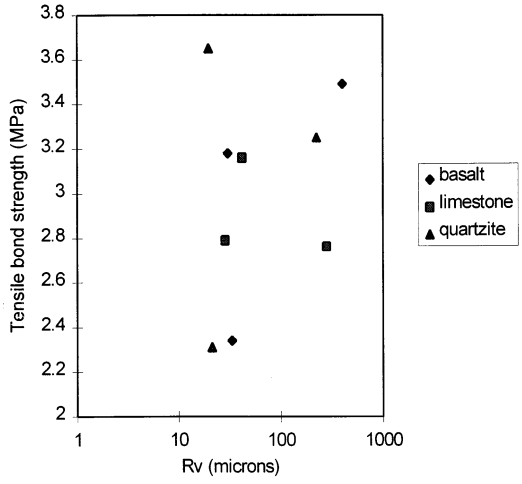

FIG. 9.

The effect of the average valley height (R_v) below the mean line of the rock aggregate surface profile on measured bond strength.

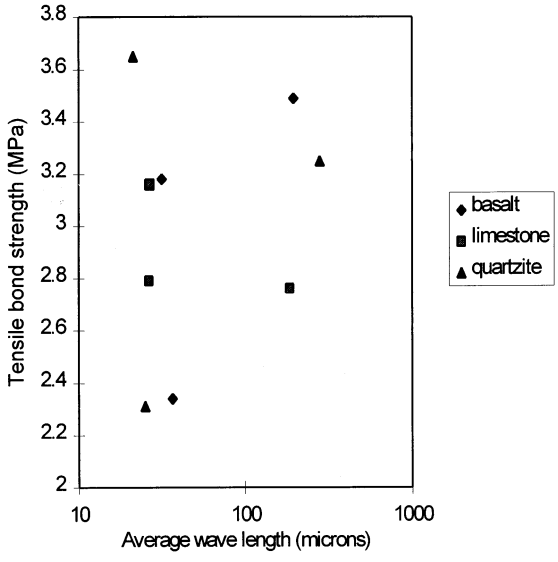

FIG. 10.

The effect of the average wavelength (λ_a) between successive peak heights within the rock aggregate surface profile on measured bond tensile strength.

the aggregate. The fractured surface achieved the least bond strength followed by the ground surface, which showed the type A failure. On the other hand, limestone and basalt aggregate-cement paste composites achieved similar bond strength with the sawn surfaces. The slightly rougher surface (Table 2) of the basalt aggregate coupled with the high porosity at the limestone ITZ (8) may have compensated for the chemical influence of limestone, and this could possibly explain why both aggregates achieved similar bond strength with sawn surfaces. In contrast to basalt aggregate, the fractured surface of limestone achieved an "apparent" bond strength value lower than that for its sawn surface and showed a type C mode of failure. Monteiro and Andrade (10) reported similar behaviour for fractured limestone when cement paste-limestone composites were tested for bond strength. Visual observation of the cleavage planes produced after bond testing revealed that, unlike in the other aggregates, the failure plane went through the weak calcite cleavage planes in the limestone aggregate. This observation indicated that although the fractured limestone surface provided a larger surface area for bonding with the cement paste compared with the sawn and the ground surfaces, a lower bond strength was achieved. This was because of the presence of large crystals of calcite, which have low bond and tensile strength on their cleavage surfaces in this rock.

Quartzite Aggregate. The nature of the quartzite aggregate-cement paste interfacial bond was significantly different from those of the basalt and limestone aggregates. The ground surface achieved the least bond strength and showed a type A mode of failure. This is probably due to the fact that its ground surface was smoother (Table 2) than the ground surfaces of basalt and limestone due to its strong internal texture. Unlike basalt and limestone, the saw-cut surface of quartzite achieved the highest "apparent" interfacial bond strength and showed a type B mode of failure. A pozzolanic reaction between Si^{4+}, leached out from quartzite (8), and the CH may possibly be the reason for this high bond strength. On the other hand, the fractured surface of quartzite achieved a lower "apparent" bond strength and showed a type D mode of failure. A combination of the smooth conchoidal fractured surface and the presence of already cracked surfaces or partially loose rock fragments (resulting from brittle fracture in this rock) at the bonded surface of this aggregate could be reasons for the low "apparent" bond strength achieved by the fractured surface. Fragments of this rock were observed on the cement paste after the test. In contrast, basalt aggregate has a firmer or stronger crystalline texture with no zones of weakness and hence higher bond strength was achieved with its fractured surface.

It is generally believed that interfacial bond strength increases with increasing surface area available for bonding (i.e. increasing roughness); however, the aggregate needs to be mechanically strong enough at its bonded surface to withstand this increase in bond strength. Figures 5 to 10 show that surface characteristics alone could not be used successfully to predict bond strength where a variety of aggregate types and surfaces are used. This suggests that differences in mechanical strength of aggregate (Table 1), internal structure, and chemical interactions (8,11) are also important parameters controlling bond strength and mode of failure at the interface. It is suggested, based on the work presented here, that the ITZ in concrete should not only concern the transition zone between the bulk cement paste and the aggregate, as currently referenced, but should also include the outer-most part of the aggregate including undulations and crevices. Hence, the interface should be modelled as a composite in its own right.

Conclusion

Measurements of surface parameters relating to aggregate surface texture showed substantial differences in topography between the three aggregates studied depending on whether the surface is sawn, ground or fractured. The "apparent" interfacial bond strength for a given cement paste, on the other hand, was found not to be a simple function of aggregate surface roughness, but also a function of parent rock structure and strength, both of which determine the topography and fracture properties of aggregates at the ITZ.

Acknowledgments

Financial support from the Centre for Cement & Concrete (CCC) at the University of Sheffield, where this work was carried out, is gratefully acknowledged. The authors would also like to thank G. Mulhearn, a member of the technical staff of the Department of Earth Sciences at the University of Sheffield, for cutting the rocks used in this investigation.

References

1. K.M. Alexander, J. Wardlaw, and D.J. Gilbert, Proc. Intl. Conf. on the Struct. of Con., Cem. Conc. Ass., London, pp 59–81, 1965.
2. T.T.C. Hsu and O.F. Slate, ACI J. 465–485, 1963.
3. J. Farran, Revue des Materiaux de Construction 490–491, 155–172 (July-August 1956), and 492, 191–209 (September 1956).
4. C.Z. Yuan and W.J. Guo, Cem. Con. Res. 17, 544–552, (1987).
5. R. Zimbelman, Cem. Con. Res. 15, 801–808, (1985).
6. P.J.M. Monteiro and P.K. Mehta, Cem. Con. Res. 16, 127 (1986).
7. M.G. Alexander, S. Mindess, S. Diamond, and L. Qu, Mater. Struct. 28, 479–506 (1995).
8. W.A. Tasong, Department of Civil & Structural Engineering. Sheffield, U.K.: University of Sheffield; Ph.D. Thesis. 1997.
9. M.G. Alexander and A. Stamatiou, Mater. Res. Soc. Symp. 367–376 (1995).
10. P.J.M. Monteiro and W. P. Andrade, Cem. Con. Res. 17, 919–926 (1987).
11. W.A. Tasong, J.C. Cripps, and C. J. Lynsdale, Cem. Con. Res. In press.